Thermodynamic functions of the $S=\frac{1}{2}$ one-dimensional ferromagnet via the renormalization-group approach and Green's function technique

L. S. Campana, A. Caramico D'Auria, U. Esposito, and G. Kamieniarz*
Dipartimento di Scienze Fisiche, Università di Napoli, Piazzale Tecchio 80, 80125 Napoli, Italy
(Received 2 May 1988; revised manuscript received 10 November 1988)

The model applicable to $(C_6H_{11}NH_3)CuBr_3$ is studied within the framework of the real-space renormalization-group approach as well as the Green's function technique. The zero-field specific heat is evaluated in the first-order generalized-cumulant expansion and qualitative agreement with the reliable numerical data and experimental results is found. Some crossover effects observed at low temperatures are also discussed. The in-plane magnetization is calculated by having recourse to the first-order Green's function approach and an instability of the spin-wave contribution under the thermal renormalization of magnons is demonstrated.

I. INTRODUCTION

Quasi-one-dimensional magnetic systems attract a great deal of interest among both theoreticians and experimentalists.[1,2] A well-known example of the system in question is $(C_6H_{11}NH_3)CuBr_3$ (CHAB) (Refs. 3 and 4) which displays magnetic order below $T_c=1.5$ K. The interchain interactions responsible for the finite T_c are weaker than intrachain interactions by a few orders of magnitude. The nonlinear excitations should play an essential role[5] in the thermodynamic properties of CHAB.

From a number of experiments[3,6–8] it has been deduced that the model Hamiltonian for CHAB has the following form:

$$H=-2J\sum_i (S_i^x S_{i+1}^x+S_i^y S_{i+1}^y+\Delta S_i^z S_{i+1}^z) \\ -g\mu_B B\sum_i S_i^x \quad (1)$$

if the magnetic field B is applied along the chain axis. In the Hamiltonian (1) $S_i^{x,y,z}$ stands for the spin-$\frac{1}{2}$ operators and the constants are defined in the standard way. The exchange integral J, the anisotropy parameter Δ, and the g factor have the following values:

$$J/k_B=55\text{ K},\quad \Delta=0.95,\quad g=2.01\ . \quad (2)$$

The Hamiltonian (1) can be mapped onto the classical sine-Gordon (sG) (Ref. 9) Hamiltonian provided that some assumptions are imposed and a well-defined peak feature of the in-plane specific heat was predicted from the numerical transfer-matrix calculations.[10] The specific-heat experimental data[4] were interpreted in terms of the sG model. However, they turned out to deviate systematically[5] from the sG predictions. A number of theoretical attempts have been undertaken to improve the classical sG model. The quantum version of the sG model[11–13] leads even to somewhat larger deviations from the experiment (for CHAB), whereas the semiclassical approach[13] improves the free-soliton picture but is inferior to that of the quantum sG model. Much better agreement with experiment was found from some numerical calculations.[14–16]

In the present paper we apply the real-space renormalization-group approach to the Hamiltonian (1) as far as the zero-field specific heat is concerned. We put $B=0$ in order to simplify our calculations. We note that the Hamiltonian (1) can be only mapped onto the sG counterpart if the in-plane field $B\neq 0$. As far as we know this is a new attempt to analyze the Hamiltonian in question. Previously the method was applied to the planar Ising-like Heisenberg model[17] and to some particular one-dimensional models.[18]

CHAB is nearly an isotropic system ($\Delta=0.95$). The symmetry of the model (1) imposes some conditions on the renormalization transformations. Our model should remain isotropic or XY type if $\Delta=1$ or $\Delta=0$, respectively. It is particularly important if we want to analyze the crossover of our nearly isotropic system towards the XY behavior which has been experimentally observed.[7] The symmetry of XY model is not preserved by the decimation transformation[19,20] so that we refer to the block method and a cumulantlike expansion. Our first-order results yield a picture which is only qualitatively correct.

Recently, some properties of CHAB (relaxation and magnetization) have been interpreted[8] in the framework of a model with free quantum magnons and free classical solitons. In the second part of the paper we show, by having recourse to the Green's function technique, that the linear-magnon contribution to the Hamiltonian (1) strongly depends on the approximations. It is striking that thermally renormalized magnons lead to the estimates which deviate significantly from the free-boson magnetization so that the hybridized magnon-soliton picture seems to be oversimplified.

Our renormalization-group approach is presented in Sec. II. A relation is also made with some numerical and experimental data. In Sec. III we develop the Green's function approach and compare our data with the known results. The paper ends with some concluding remarks.

II. RENORMALIZATION-GROUP APPROACH

In the present section some zero-field thermodynamic quantities are calculated by having recourse to the real-space renormalization-group (RSRG) approach. The model Hamiltonian (1) is transformed into the form

$$-\beta H=\tfrac{1}{2}K\sum_{j=1}^{N}(\sigma_j^x\sigma_{j+1}^x+\sigma_j^y\sigma_{j+1}^y)+\tfrac{1}{2}K_z\sum_{j=1}^{N}\sigma_j^z\sigma_{j+1}^z\ , \tag{3}$$

where

$$K=J/k_BT,\quad K_z=\Delta K \tag{4}$$

and $\sigma_j^{x,y,z}$ stand for the spin-$\frac{1}{2}$ Pauli operators.

We divide the chain into N' cells consisting of $n_s=3$ sites and introduce cell-spin Pauli operators $\mathbf{S}_i$ for each cell. The renormalization transformation preserving the free energy is defined[17,21] by

$$\exp[-\beta' H'(\mathbf{S})]=\mathrm{Tr}_\sigma\exp[-\beta H(\sigma)]P(\mathbf{S},\sigma)\ . \tag{5}$$

The weight operator $P(\mathbf{S},\sigma)$, which links the site spins and the cell spins, can be considered as the extension[17,22] to the quantum systems of the weight function introduced for the classical Ising model.[21] If the weight operator has a higher degree of symmetry, different types of Hamiltonians can be treated within the same transformation. Usually, the following rotationally invariant form is chosen:

$$P(\mathbf{S},\sigma)=\prod_{i=1}^{N'}\tfrac{1}{2}[1+\tfrac{1}{2}\mathbf{S}_i\cdot\mathbf{M}(\sigma_{im})]\ , \tag{6}$$

where the operator $\mathbf{M}(\sigma_{im})$ can be defined according to Sznajd[22] [hereafter referred to as the Sznajd **M** operator (SMO)] or Brower *et al.*[17] (BMO).

In order to perform the trace operation in (5), we divide the Hamiltonian (3) into an intracell term H^0 and an intercell term V, and we expand the corresponding exponential in terms of V via the Baker-Campbell-Hausdorf (BCH) formula[23] or the Feynman expansion.[17] The results presented here have been found for both operators $\mathbf{M}(\sigma_{im})$ and for both types of expansions. Up to the first order, the renormalized Hamiltonian H' preserves the original form with an extra constant term $N'\ln Z$. The renormalized parameters are given by

$$K'=K(\rho/Z)^2,\quad K_z'\equiv\Delta' K'=K_z(\rho_z/Z)^2\ , \tag{7}$$

where ρ, ρ_z, and Z are reported in the Appendix.

The renormalization-group transformations (7) fulfill the isotropic symmetry if $\Delta=1$. In that case BCH and Feynman expansion give the same result,

$$\rho=\rho_z=(10/9)\exp(K)+b\exp(-2K)\ , \tag{8}$$

where $b=\frac{8}{9}$ or $\frac{6}{9}$ for SMO or BMO, respectively. The transformations (7) have no nontrivial fixed points. We find only the following fixed-point solutions: $(K^*,K_z^*)=(\infty,\infty)$ (the isotropic Heisenberg fixed point at $T=0$), $(K^*,K_z^*)=(\infty,0)$ (the XY fixed point at $T=0$) as well as $(K^*,K_z^*)=(0,0)$; the latter is attractive.

TABLE I. The correlation length exponent ν for the Heisenberg ($\Delta=1$) and XY ($\Delta=0$) models.

	$\Delta=1$	$\Delta=0$	
		SMO	BMO
BCH	0.93	1.64	1.68
Feynman	0.93	0.652	0.665

There exists a definite limit of (7) at $T=0$ which for $\Delta<1$ gives $\Delta'<\Delta$, so that there is a flow line from the isotropic fixed point towards the XY fixed point at $T=0$, and the exact result is recovered.[24] However, we cannot linearize the recursion relations (7) around the trivial isotropic fixed point at $T=0$ in the two-parameter space (K,K_z) since they have an analytic form $\exp(1/T)$. It is likely that in this way the essential singularity[24] at the point $\Delta=1$ is manifested in our approach. In the one-parameter subspace $K=K_z$ or $K_z=0$ the transformations (7) can be linearized in terms of the variable $t=1/K$ around $t^*=0$ and the corresponding correlation length exponents ν are reported in Table I. The exact result[20,25] for ν is $\nu=1$. We see that in the XY limit our results are not accurate. They depend strongly on the type of expansion and only slightly on the choice of the **M** operators.

In Fig. 1 we present, in the logarithmic scale, the flow lines which follow from the recursion relations (7) if they are iterated. For all the curves (apart from that drawn in the continuous line) the starting point corresponds to $\Delta=0.95$ and temperature is fixed via (4) by the value $K^{(0)}$ indicated explicitly. Having chosen $\Delta=0.95$, we refer to the physical system to CHAB. The continuous curve denoted by $\Delta=0.25$ is not a flow line but it represents the function $y=0.25K$. All the flow lines are attracted by the stable fixed point $(K^*=0,\ K_z^*=0)$ but only the ones corresponding to temperatures low enough enter the region below the continuous curve. The value $\Delta=0.25$ is closer to the XY limit ($\Delta=0$) than to the isotropic limit

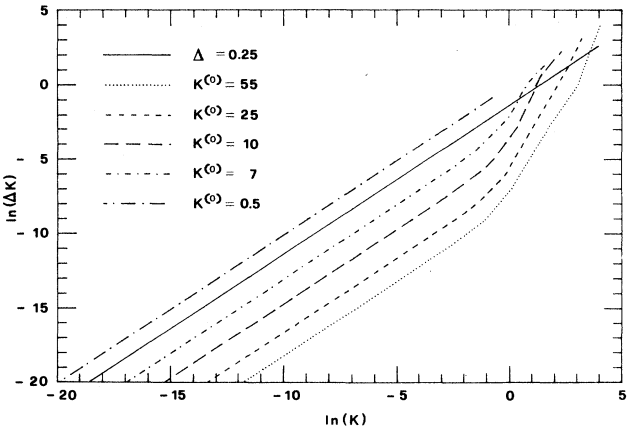

FIG. 1. Flow-line picture in the logarithmic scale. The solid line represents the function $y=0.25K$, whereas the remaining curves depict the flow lines starting from $\Delta=0.95$ and $K^{(0)}$ as indicated in the figure.

($\Delta=1$) so that we could expect that, when the flow lines enter the region below the continuous line in Fig. 1, our nearly isotropic physical system should display the XY-like behavior as far as the critical phenomena are concerned. According to the data represented in Fig. 1, this crossover should appear in the region $0.5K_{\rm cross}<7$. If we define the curve $y=\alpha K$ as the separatrix of our parameter space, we should expect the XY-like behavior when the system flows into the region below αK for α small enough. The α dependence of the inverse crossover temperature $K_{\rm cross}$ is shown in Fig. 2. We see that $K_{\rm cross}$ amounts to about 4.5 or 5.5 for $\alpha=0.25$ or 0.10, respectively. Since $\alpha=0.10$ is much lower than 1, we can estimate the crossover temperature $T_{\rm cross}\lesssim 10K$. Our estimate of the crossover temperature is rather well confirmed ($T_{\rm cross}\simeq 4K$) by the neutron scattering experiment[8] on CHAB. We have presented this qualitative analysis, referring to the Feynman identity. The analysis based on the BCH expansion leads to a flow-line picture which has the same qualitative behavior as that shown in Fig. 1. However, the estimates of $K_{\rm cross}$ remain practically unaltered. An indication of the crossover behavior was found in some numerical calculations,[16] but our present discussion demonstrates the crossover more directly. As it was mentioned above, we cannot linearize our recursion relations near $T=0$ in the two-parameter space, so that our analysis is not performed in terms of the scaling function[20] but referring to the flow-line picture.

In the remaining part of this section, the specific heat of the system (3) is evaluated as the corresponding derivative of the free energy. The free energy per spin can be calculated by iterating the renormalization process and summing up all the constant terms which emerge in the renormalization procedure so that

$$f=\sum_{p=0}^{\infty}(\ln Z_p)/n_s^{p+1}\ , \tag{9}$$

where Z_p is the cell partition function after p renormalization steps. The specific heat can be expressed in terms of the free energy as

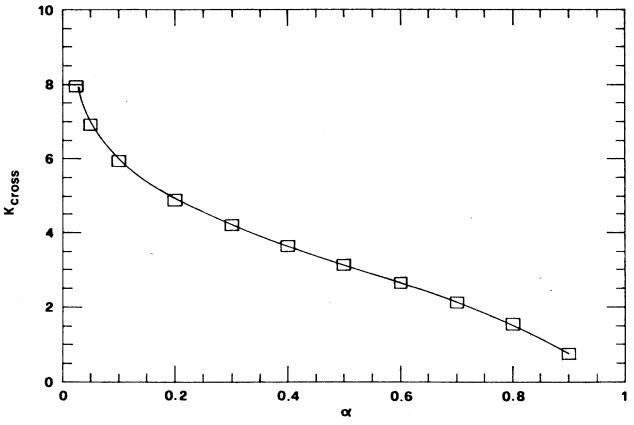

FIG. 2. The inverse crossover temperature $K_{\rm cross}$ vs a parameter α which specifies the XY region.

$$C=K^2\frac{\partial^2 f}{\partial K^2}\ . \tag{10}$$

Our final results are presented in Fig. 3 for $\Delta=0$, $\Delta=0.95$, and $\Delta=1$. The dotted curves represent the estimates we find by having recourse to the BCH formula, and the dashed lines represent the corresponding estimates based on the Feynman expansions. Both types of expansion give the same result in the isotropic limit $\Delta=1$, and the corresponding data are reported by a chain line. Our data are compared with the exact results[26] for the XY model, which are represented in Fig. 3 by the triangles. The squares and circles display the numerical estimates[27] for $\Delta=0.95$ and $\Delta=1$, respectively. The latter are very accurate for $k_BT/J\gtrsim 0.2$ and were used in a fit of the experimental data[3] which lead to the parameters listed in (2) for CHAB.

We find that an overall agreement with the exact and numerical data is much better if the Feynman expansion is used, in particular at low temperatures. At higher temperatures both expansions lead to the same results. We attribute this drastic difference at low T to the following fact: The Feynman expansion is given strictly in terms of V, whereas the BCH formula yields the perturbation terms which are considered according to the power of K. Although we have not accomplished to recover quantitatively the exact or numerical results in the entire temperature region, our results (based on the Feynman expansion) demonstrate all the essential features at least qualitatively. In particular, we find that the peak positions and the peak heights of the specific heat are rather well represented. Again, both **M** operators lead to similar estimates and those presented in Fig. 3 are obtained for SMO.

III. GREEN'S FUNCTION APPROACH

In this section the magnetization of the model (1) will be calculated in the framework of a Green's function technique. Our Zubarev's[28] temperature-dependent Green's functions are defined in Ref. 29, and hereafter we follow the notation introduced therein. The model Hamiltonian we consider here can be written in terms of the spatial Fourier transforms $S_k^{\pm}$ and S_k^z of the spin operators $S_i^{\pm}, S_i^z$ in the following way:

$$\begin{aligned}H=&-g\mu_B BS_{k=0}^z\\&-\frac{1}{N}\sum_k[(J^{xx}+J^{yy})\gamma_k S_k^+S_k^-\\&\quad+\tfrac{1}{2}(J^{xx}-J^{yy})\gamma_k(S_k^+S_{-k}^+ +S_k^-S_{-k}^-)\\&\quad+2J^{zz}\gamma_k S_k^zS_{-k}^z]\ ,\end{aligned} \tag{11}$$

where

$$J(k)=\sum_j J_{ij}^{ik(l-j)}=\gamma_k J(0) \tag{12}$$

and J^{xx}, J^{yy}, and J^{zz} are the exchange parameters as introduced in Ref. 8. If $J^{xx}=J^{zz}$ and $J^{yy}/J^{xx}=0.95$, we obtain the model equivalent to (1). The anisotropy[8] in the xz easy plane is very weak ($J^{zz}/J^{xx}=0.9995$) and the

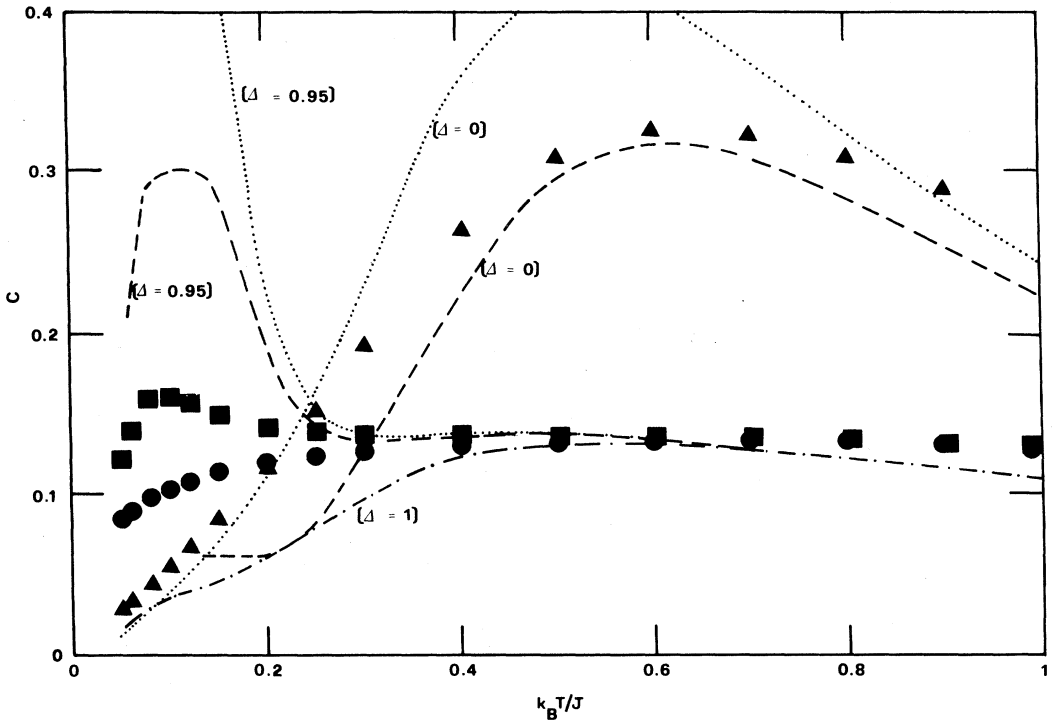

FIG. 3. The dimensionless specific heat per spin vs the reduced temperature k_BT/J. The dotted curves report our results obtained from the BCH formula whereas the dashed curves—those from the Feynman identity. The values of Δ specify the anisotropy. The chain line represents our results in the isotropic limit. The exact data for the XY model are depicted by the triangles and the corresponding numerical data for $\Delta=0.95$ and $\Delta=1$ by the squares and circles, respectively.

magnetic field $B=0.5$ kG is sufficient to align spins along the z axis. [There is a misprint in Eq. (13) of Ref. 8 in the case B parallel to c axis. J^{zz} should be read as J^{xx}.] The experiments[8] we refer to were performed in the region $B \gtrsim 10$ kG, so that we assume the ground-state spin configuration in the z direction.

The quantities Ω_{11}^k and Ω_{12}^k (details are given in Ref. 29) which determine the energy spectrum ω_k of the undamped linear excitations

$$\omega_k=[(\Omega_{11}^k)^2-(\Omega_{12}^k)^2]^{1/2} \tag{13}$$

depend on the decoupling procedures. In the simple random-phase approximation RPA approximation we find

$$\begin{aligned}\Omega_{11}^k&=h+4\sigma J^{zz}-2\sigma(J^{xx}+J^{yy})\gamma_k\ ,\\ \Omega_{12}^k&=-2\sigma(J^{xx}-J^{yy})\gamma_k\ ,\end{aligned} \tag{14}$$

where $h=g\mu_BB$ and $\sigma=\langle S_i^z\rangle$. If the magnetization σ in (14) is replaced by $\frac{1}{2}$, the free-boson approximation[8] is recovered.

Usually[29–31] thermodynamic quantities can be improved with respect to RPA within a spectral-density method (SDM). In that case an implicit decoupling is performed in such a way that the spectral density preserves the first two moments. We find then

$$\begin{aligned}\Omega_{11}^k&=h+\frac{1}{2\sigma N^2}\sum_q\gamma_q\{4[2J^{zz}-(J^{xx}+J^{yy})\gamma_k]\langle S_q^zS_{-q}^z\rangle+2(J^{xx}+J^{yy}-2J^{zz}\gamma_k)\langle S_q^-S_q^+\rangle+2(J^{xx}-J^{yy})\langle S_q^-S_{-q}^-\rangle\}\ ,\\ \Omega_{12}^k&=\frac{1}{2\sigma N^2}\sum_q\gamma_q[2(J^{xx}+J^{yy}-2J^{zz}\gamma_k)\langle S_q^+S_{-q}^+\rangle+2(J^{xx}-J^{yy})\langle S_q^-S_q^+\rangle-4(J^{xx}-J^{yy})\gamma_k\langle S_q^zS_{-q}^z\rangle]\ .\end{aligned} \tag{15}$$

As before,[29] the coupled sets (15) and (13) can be solved if the RPA-like decoupling is assumed for the longitudinal correlation function

$$\langle S_q^zS_{-q}^z\rangle=\langle S_q^z\rangle\langle S_{-q}^z\rangle \tag{16}$$

as well as the spectral theorem is applied in order to calculate the corresponding transverse spin correlation functions.

The final set of equations we solve numerically, has the form

$$C_1=\frac{1}{N}\sum_q \gamma_q R_q \coth(\beta\omega_q/2)\ ,$$

$$C_2=\frac{1}{N}\sum_q \gamma_q R_q^{-1}\coth(\beta\omega_q/2)\ , \tag{17}$$

$$\sigma^{-1}=\frac{1}{N}\sum_q (R_q+R_q^{-1})\coth(\beta\omega_q/2)\ ,$$

where

$$R_q=[(\Omega_{11}^k-\Omega_{12}^k)/(\Omega_{11}^k+\Omega_{12}^k)]^{1/2}\ ,$$
$$\Omega_{11}^k+\Omega_{12}^k=h+4\sigma(J^{zz}-J^{xx}\gamma_k)+2(J^{xx}-J^{zz}\gamma_k)C_1\ , \tag{18}$$
$$\Omega_{11}^k-\Omega_{12}^k=h+4\sigma(J^{zz}-J^{yy}\gamma_k)+2(J^{yy}-J^{zz}\gamma_k)C_2$$

and the corresponding results for magnetization are reported in Fig. 4.

In Fig. 4 the continuous curve denoted as the total represents the predictions of the heuristic model[8] with free quantum spin-wave excitations and nonlinear classical soliton excitations. The soliton contribution is drawn by a dotted line after Ref. 8. Our result for the magnon contribution to the reduced magnetization $M=2\sigma$ is reported by circles and by the dashed line and coincides with that found before.[8] It turns out that the continuous curve gives a good representation of the experimental data,[8] so that hereafter we refer to that as to the experimental results.

Some recent numerical calculations[32,33] confirm that these experimental data can be explained by the model (1), so that it is interesting to check whether this picture with free magnons, when the magnetization is reduced by a factor 2 with respect to the saturation value, can be supported by the theory which should be valid in a more extended region of temperatures. Our picture with the thermally renormalized spin waves leads to the data reported in Fig. 4 by the triangles and squares for the RPA and SDM approximations, respectively. They are close to those of the boson approximation in the low-temperature limit, but they display significant deviations

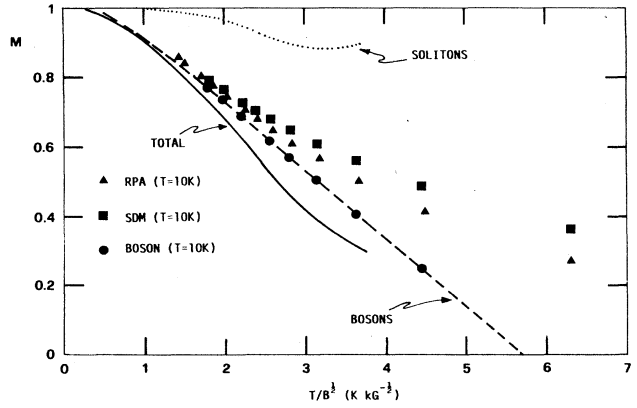

FIG. 4. The reduced magnetization M as a function of $T/\sqrt{B}$. Our results are shown by the circles (boson approximation), triangles (RPA), and squares (SDM). The dashed curve interpolates the corresponding data. The dotted and solid lines describe a soliton contribution and the experimental data on CHAB (Ref. 8).

at higher temperatures where the solitons are activated. Within SDM the deviations from the free-boson model exceed the estimated soliton contribution.[8] In both cases (RPA and SDM) the thermal effects enlarge the deviations of the theoretical results from the experimental data, and the corresponding increase cannot be neglected with respect to the soliton contribution.

We have already found[31] the increase of the magnetization with respect to the boson approximation, applying SDM to the isotropic classical model. However, in that case our predictions turned out to agree with some exact transfer-matrix calculations[34] in the temperature region where the interacting boson approximation failed.

We point out that SDM predictions were also very well supported by the reliable high-temperature expansion[35] as far as the $T=0$ critical field is concerned for the Ising model with a transverse field.[29] The transverse Ising model is a quantum model but displays a quantum critical behavior only at $T=0$. At finite temperature the usual critical behavior of the classical Ising model is predicted.[36] We end up with the conclusion that the deviations of our SDM calculations from the experimental data demonstrate an essential role of the quantum effects for the model in question.

IV. DISCUSSION

We have supplemented the theoretical studies of the easy plane system (1) by the RSRG approach and the Green's function technique (RPA and SDM). We have shown that our first-order RSRG scheme based on the Feynman identity yields the estimates of the zero-field specific heat which are consistent with the exact results for the XY model,[26] the numerical results,[27] and the corresponding experimental data. At low temperatures, the deviations are of the order of 100%, whereas at higher temperatures they are reduced to 10–20%. However, the peak positions and peak heights are rather well represented in the intermediate temperature range. Our first-order predictions are not inferior to those found in the framework of the sine-Gordon model.[12–13,37,38] We also note that surprisingly good agreement between the numerical calculations[39] and simple RSRG truncation method results shown in Fig. 1 of Ref. 18 are fortuitous. This method fails when applied to our ferromagnetic model (1). It is also hopeless to try to extend our previous approach[40,41] for the quantum Ising model unless the proper weight operator is introduced.

We have extended the RSRG analysis to the crossover effects observed experimentally for CHAB.[7] Our qualitative discussion based on the flow-line picture yields the estimate $T_{\rm cross}\lesssim 10K$ which is well confirmed ($T_{\rm cross}\simeq 4K$) by the experiment.

In view of the recent conjecture[8] on the role of the free magnons and solitons in the temperature region which is normally not accessible for the spin-wave description, we have performed some calculations of the magnetization by having recourse to the Green's function approach. In contrast to our previous estimates[31] for the classical model, we find significant deviations from the experimental[8] and numerical results.[32–33] The deviations we encounter

are of the order of the estimated soliton contribution, so that we have demonstrated that the model in question is unstable under the thermal renormalization of magnons. Our results may also indicate that the physical picture which follows from the semiclassical approach[13] is oversimplified. According to that picture, classical solitons present in the system modify the linear spin waves, but this is only reflected by a shift in the phase of the spin waves. It seems that the role of the thermal effects has not been sufficiently taken into account.

ACKNOWLEDGMENTS

We wish to thank Professor R. Dekeyser for many discussions and turning our attention to the crossover analysis in terms of the flow-line picture, Dr. J. Sznajd for his explanation about the quantum weight operator, Dr. C. Vanderzande for some suggestions and discussions, and Dr. P. Lo Re for his assistance in the numerical computations. G.K. would like also to thank the Institute of Physics of the Lodz University for a partial support via project CPBP 01.08.

APPENDIX

The cell partition function Z which appears in the constant term of the renormalized Hamiltonian is given by

$$Z=\sum_{\alpha=1}^{4}\exp(-\beta\varepsilon_\alpha)=\sum_{\alpha=1}^{4}\zeta_\alpha\ , \tag{A1}$$

where

$$\begin{aligned}&-\beta\varepsilon_1=\Delta K,\quad \varepsilon_2=0,\quad -\beta\varepsilon_3=\frac{K}{2}(-\Delta+\delta)\ ,\\ &-\beta\varepsilon_4=\frac{K}{2}(-\Delta-\delta)\ ,\end{aligned} \tag{A2}$$

$$\delta=(\Delta^2+8)^{1/2}\ . \tag{A3}$$

For the BCH expansion ρ and ρ_z are given by

$$\begin{aligned}\rho&=\tfrac{1}{3}\zeta_1+f_+\zeta_3+f_-\zeta_4\ ,\\ \rho_z&=\zeta_1+g_-\zeta_3+g_+\zeta_4\ ,\end{aligned} \tag{A4}$$

where for the SMO

$$\begin{aligned}f_\pm&=\tfrac{1}{6}[5\pm(\Delta-2)/\delta]\ ,\\ g_\pm&=\tfrac{1}{6}[3\pm(3\Delta+4)/\delta]\end{aligned} \tag{A5}$$

and for BMO

$$\begin{aligned}f_\pm&=\tfrac{1}{18}(13\pm3\Delta/\delta)\ ,\\ g_\pm&=\tfrac{1}{18}[7\pm(7\Delta+8)/\delta]\ .\end{aligned} \tag{A6}$$

For the Feynman expansion ρ_z is given by

$$\begin{aligned}\rho_z^2=C_1^2&+2C_2^2\zeta_3\zeta_4+4C_1C_2\zeta_3\phi[\beta(\varepsilon_3-\varepsilon_4)]\\ &+2C_2^2\zeta_3^2\phi[2\beta(\varepsilon_3-\varepsilon_4)]\ ,\end{aligned} \tag{A7}$$

where

$$C_1=\zeta_1+\alpha_-\gamma_-\zeta_3+\alpha_+\gamma_+\zeta_4,\quad C_2=\gamma(\Delta-1)/\delta^2\ , \tag{A8}$$

$$\gamma_\pm=\tfrac{1}{2}(1\pm\Delta/\delta),\quad \phi(x)=(e^x-1)/x \tag{A9}$$

and for SMO

$$\alpha_\pm=\tfrac{1}{6}[5\pm(\Delta+8)/\delta],\quad \gamma=-\tfrac{2}{3}\ , \tag{A10}$$

whereas for BMO

$$\alpha_\pm=\tfrac{1}{9}[6\pm(\Delta+8)/\delta],\quad \gamma=-\tfrac{4}{3}\ . \tag{A11}$$

The expression for ρ is the following:

$$\begin{aligned}\rho^2=&D_1^2+2(D_2^2\zeta_1\zeta_3+D_3^2\zeta_1\zeta_4+D_4^2\zeta_3\zeta_4)+4D_1\{D_2\zeta_1\phi[\beta(\varepsilon_1-\varepsilon_3)]+D_3\zeta_1\phi[\beta(\varepsilon_1-\varepsilon_4)]+D_4\zeta_3\phi[\beta(\varepsilon_3-\varepsilon_4)]\}\\ &+2\{D_2^2\zeta_1^2\phi[2\beta(\varepsilon_1-\varepsilon_3)]+D_3^2\zeta_1^2\phi[2\beta(\varepsilon_1-\varepsilon_4)]+D_4^2\zeta_3^2\phi[2\beta(\varepsilon_3-\varepsilon_4)]\}\\ &+4D_2D_3\{\zeta_1^2\phi[\beta(2\varepsilon_1-\varepsilon_3-\varepsilon_4)]+\zeta_1\zeta_3\phi[\beta(\varepsilon_3-\varepsilon_4)]\}+4D_2D_4\{\zeta_3^2\phi[\beta(2\varepsilon_3-\varepsilon_1-\varepsilon_4)]+\zeta_1\zeta_3\phi[\beta(\varepsilon_1-\varepsilon_4)]\}\\ &+4D_3D_4\{\zeta_4^2\phi[\beta(2\varepsilon_4-\varepsilon_1-\varepsilon_3)+\zeta_3\zeta_4\phi[\beta(\varepsilon_3-\varepsilon_1)]\}\ ,\end{aligned} \tag{A12}$$

where

$$D_1=\frac{2}{\delta}(\alpha_x\zeta_3-\beta_x\zeta_4),\quad D_2=\tfrac{1}{6}[1+(\Delta+2)/\delta]\ , \tag{A13}$$

$$D_3=\tfrac{1}{6}[1-(\Delta+2)/\delta],\quad D_4=\Gamma_x\Delta(\Delta-1)/\delta^2\ , \tag{A14}$$

and for the SMO

$$\begin{aligned}\alpha_x&=-\tfrac{1}{3}[1-(\Delta+8)/\delta]\ ,\\ \beta_x&=-\tfrac{1}{3}[1+(\Delta+8)/\delta],\quad \Gamma_x=\tfrac{2}{3}\ ,\end{aligned} \tag{A15}$$

while for the BMO

$$\begin{aligned}\alpha_x&=-\frac{1}{6}\left[1-\frac{5}{3}\frac{(\Delta+8)}{\delta}\right]\ ,\\ \beta_x&=-\frac{1}{6}\left[1+\frac{5}{3}\frac{\Delta+8}{\delta}\right],\quad \Gamma_x=\tfrac{5}{9}\ .\end{aligned} \tag{A16}$$

*On leave of absence from the Institute of Physics, A. Mickiewicz University, 60-769 Poznan, Poland.

[1]*Magnetic Excitations and Fluctuations,* edited by S. W. Lovesey, U. Balucani, F. Borsa, and V. Tognetti (Springer-Verlag, Heidelberg, 1984).

[2]*Magnetic Excitations and Fluctuations II,* edited by U. Balucani, S. W. Lovesey, M. G. Rasetti, and V. Tognetti (Springer-Verlag, Heidelberg, 1987).

[3]K. Kopinga, A. M. C. Tinus, and W. J. M. de Jonge, Phys. Rev. B **25**, 4685 (1982).

[4]K. Kopinga, A. M. C. Tinus, and W. I. M. de Jonge, Phys. Rev. B **29**, 2868 (1984).

[5]A. M. C. Tinus, W. J. M. de Jonge, and K. Kopinga, Phys. Rev. B **32**, 3154 (1985).

[6]A. C. Phaff, C. H. W. Swüste, W. J. M. de Jonge, R. Hoogerbeerts, and A. J. van Duyneveldt, J. Phys. C **17**, 2583 (1984).

[7]K. Kopinga, W. J. M. de Jonge, M. Steiner, G. C. de Vries, and E. Frikkee, Phys. Rev. B **34**, 4826 (1986).

[8]K. Kopinga, A. M. C. Tinus, W. J. M. de Jonge, and G. C. de Vries, Phys. Rev. B **36**, 5398 (1987).

[9]E. Magyari and H. Thomas, J. Phys. C **15**, L333 (1982).

[10]T. Schneider and E. Stoll, Phys. Rev. B **22**, 5317 (1980).

[11]M. Fowler and X. Zotos, Phys. Rev. B **25**, 5806 (1982).

[12]M. D. Johnson and N. F. Wright, Phys. Rev. B **32**, 8798 (1985).

[13]H. C. Fogedby, K. Osano, and H. J. Jensen, Phys. Rev. B **34**, 3462 (1986).

[14]I. Satija, G. Wysin, and A. R. Bishop, Phys. Rev. B **31**, 3205 (1985).

[15]G. Kamieniarz and C. Vanderzande, Phys. Rev. B **35**, 3341 (1987).

[16]G. Kamieniarz, Phys. Rev. B **38**, 4873 (1988).

[17]R. C. Brower, F. Kuttner, M. Nauenberg, and K. Subbarao, Phys. Rev. Lett. **38**, 1231 (1977).

[18]A. L. Stella, C. Vanderzande, and R. Dekeyser, Phys. Rev. B **27**, 1812 (1983).

[19]M. Suzuki and H. Takano, Phys. Lett. **69A**, 426 (1979).

[20]R. B. Stinchcombe, J. Phys. C **14**, 397 (1981).

[21]Th. Niemeijer and J. M. J. van Leeuwen, Physica **71**, 17 (1974).

[22]J. Sznajd, Z. Phys. B **62**, 349 (1986).

[23]R. M. Wilcox, J. Math. Phys. **8**, 962 (1967).

[24]J. C. Bonner and G. Müller, Phys. Rev. B **29**, 5216 (1984).

[25]T. Tonegawa, Solid State Commun. **40**, 983 (1981).

[26]S. Katsura, Phys. Rev. **127**, 1508 (1962).

[27]H. W. J. Blöte, Physica **79B**, 427 (1975).

[28]D. N. Zubarev, Usp. Fiz. Nauk **71**, 71 (1960) [Sov. Phys. Usp. **3**, 320 (1960)].

[29]G. Kamieniarz, Acta Phys. Pol. **A52**, 243 (1977).

[30]U. Esposito, in *Quantum Field Theory and Quantum Statistics,* edited by I. A. Batalin, C. J. Isham, and G. A. Vilkovisky (Adam Hilger, Bristol, 1987).

[31]L. S. Campana, A. Caramico D'Auria, M. D'Ambrosio, U. Esposito, L. De Cesare, and G. Kamieniarz, Phys. Rev. B **30**, 2769 (1984).

[32]G. Kamieniarz, Solid State Commun. **66**, 229 (1988).

[33]G. Kamieniarz, F. Mallezic, and R. Dekeyser, Phys. Rev. B **38**, 6941 (1988).

[34]U. Balucani, M. G. Pini, V. Tognetti, and A. Rettori, Phys. Rev. B **26**, 4974 (1982).

[35]J. Oitmaa and G. J. Coombs, J. Phys. C **14**, 143 (1981).

[36]M. Suzuki, Prog. Theor. Phys. **56**, 1454 (1976).

[37]H. J. Mikeska and H. Frahm, J. Phys. C **19**, 3203 (1986).

[38]R. Giachetti and V. Tognetti, Phys. Rev. B **36**, 5512 (1987).

[39]J. C. Bonner and M. E. Fisher, Phys. Rev. A **135**, 640 (1964).

[40]G. Kamieniarz, L. S. Campana, A. Caramico D'Auria, and U. Esposito, J. Phys. C **20**, 1337 (1987).

[41]L. S. Campana, A. Caramico D'Auria, U. Esposito, and G. Kamieniarz, J. Phys. C **20**, 5161 (1987).